ENSO signal propagation detected by wavelet coherence and mean phase coherence methods

S.Jevrejeva[1], J.C. Moore[2], and A. Grinsted[2,3]

[1] Proudman Oceanographic Laboratory, Liverpool, UK, sveta@pol.ac.uk
[2] Arctic Centre, University of Lapland, Rovaniemi, Finland, jmoore@ulapland.fi
[3] Dept. of Geophysics, University of Oulu, Oulu, Finland, ag@glaciology.net

Abstract. We present observational evidence of the dynamic linkages between ENSO and Northern Hemisphere (NH) ice conditions over the past 135 years. Using Wavelet Transform (WT) we separate statistically significant components from time series and demonstrate significant co-variance and consistent phase differences between NH ice conditions and the Arctic Oscillation and Southern Oscillation indices (AO and SOI) at 2.2, 3.5, 5.7 and 13.9 year periods. To study the phase dynamics of weakly interacting oscillating systems we apply average mutual information and mean phase coherence methods. Phase relationships for the different frequency signals suggest that there are several mechanisms for distribution of the 2.2-5.7 year and the 13.9 year signals. The 2.2- 5.7 year signals, generated about three months earlier in the tropical Pacific Ocean, are transmitted via the stratosphere, and the Arctic Oscillation (AO) mediating propagation of the signals. In contrast the 13.9 year signal propagates from the western Pacific as eastward propagating equatorial coupled ocean waves, and then fast boundary waves along the western margins of the Americas to reach both polar regions, and has a phase difference of about 1.8-2.1 years by the time it reaches the Arctic.

1 Motivation

The impact of El Niño Southern Oscillation (ENSO) on global climate is ubiquitous, irregular, and largely unpredictable as both oceanic and atmospheric pathways are involved, resulting in considerable weakening of signal/noise ratio. There considerations motivated us to apply new nonlinear techniques (average mutual information and mean phase coherence methods) in order to detect complex and sufficiently weak nonlinear interactions. Several studies indicate that the impact of ENSO on NH climate is not robust, but is more plausibly seen during winter (Pozo-Vázquez, Esteban-Parra, Rodrigo, and Castro-Diez, 2001). Most evidence on teleconnections comes from model simulations (e.g. Merkel and Latif, 2002) or from 50 years of reanalysis data (Ribera and Mann, 2002). We use observational data of NH ice conditions to trace the ENSO signal propagation; since ice extent is an integrated pa-

rameter of winter seasons and in addition acts as a nonlinear filter for 2-13 year oscillations (Jevrejeva and Moore, 2001). Previously oscillations with 2.2, 3.5, 5.7 and 13.9 year periodicities have been detected in ice conditions time series and associated with similar signals in SOI/Niño3 and the NH annular mode (NAM) (Jevrejeva and Moore, 2001; Jevrejeva, Moore and Grinsted, 2003). Results are consistent with quasi-biennial (QB) and quasi- quadrennial (QQ) signals detected by (Gloersen, 1995; Venegas and Mysak, 2000) in shorter time series of ice conditions in polar regions and with signals in SST and sea level pressure (SLP) anomalies over the Pacific Ocean (Huang, Higuchi and Shabbar, 1998; Torrence and Webster, 1999; White and Tourre, 2003, Ribera and Mann, 2002).

The main aim of this paper is to investigate the dynamic connections between the ENSO and NH ice conditions; and to estimate how strong future evolution of one system's phase depends on the other system's phase.

2 Methods

We used the Continues Wavelet Transform (CWT) (Foufoula-Georgiou and Kumar, 1995) to determine both the dominant modes of variability and how those modes vary in time. Two useful wavelets are the Morlet (Foufoula-Georgiou and Kumar, 1995), defined as

$$\psi_0(\eta) = \pi^{-1/4} e^{i\omega_0\eta} e^{-\frac{1}{2}\eta^2} \quad , \tag{1}$$

and the Paul (Torrence and Compo, 1998):

$$\psi_0(\eta) = \frac{2^m i^m !}{\sqrt{\pi(2m)!}} (1 - i\eta)^{-(m+1)}, \tag{2}$$

where $\omega_0$is dimensionless frequency and η is dimensionless time, and m is the order, taken as 4 here. The idea behind the CWT is to apply the wavelet as a band pass filter to the time series. The wavelet is stretched in time, t, by varying its scale (s), so that $\eta = s \cdot t$, and normalizing it to have unit energy. The Morlet wavelet (with ω_0=6) provides a good balance between time and frequency localization and is a good choice for feature extraction. For broad band pass filtering applications, we use the Paul as this is much less localized in frequency space. The CWT of a time series X, $\{x_n, n=1,\ldots,N\}$ with uniform time steps δt, is defined as the convolution of x_n with the scaled and normalized wavelet.

$$W_n^X(s) = \sqrt{\frac{\delta t}{s}} \sum_{n'=1}^{N} x_{n'} \psi_0\left[(n' - n)\frac{\delta t}{s}\right]. \tag{3}$$

The complex argument of $W^X_n(s)$ can be interpreted as the phases of $X\{\phi_1 \ldots, \phi_n\}$.

We define (Grinsted, Moore and Jevrejeva, 2004) the wavelet coherence of two time series *X* and *Y*{y_1, …y_n} as

$$R_n^2(s) = \frac{\left|S\left(s^{-1}W_n^{XY}(s)\right)\right|^2}{S\left(s^{-1}\left|W_n^X(s)\right|^2\right)\cdot S\left(s^{-1}\left|W_n^Y(s)\right|^2\right)}, \quad (4)$$

where *S* is a smoothing operator. Notice that this definition closely resembles that of a traditional correlation coefficient, and it is useful to think of the wavelet coherence as a localized correlation coefficient in time frequency space. The smoothing operator $S(W) = S_{scale}(S_{time}(W_n(s)))$, where S_{scale} denotes smoothing along the wavelet scale axis and S_{time} smoothing in time. We apply Monte Carlo methods using a red noise model based on the autocorrelation functions of the two time series to provide statistical significance (Grinsted et al., 2004).

We also consider that nonlinear interactions between the two time series may be chaotic. Causality relationships are analysed using average mutual information (Papoulis, 1984) and the mean phase coherence (Mokhov and Smirnov, 2006) methods. Both these methods rely on the phase expression of the time series derived from (3) with the Paul wavelet (2) of the desired Fourier wavelength, $\lambda = 4\pi s/(2m+1)$, (Torrence and Compo, 1998). The broadband Paul wavelet allows signals that are relatively aperiodic to be included in the analysis. We utilize the average mutual information, *I(X,Y)*, between the two series. In our case we are interested in causative relations, so it is appropriate to measure the *I(X,Y)*, between their respective phases ϕ , and θ.

$$I(X,Y) = \frac{1}{\log_2 B}\sum_{y\in Y}\sum_{x\in X} p(\phi,\theta)\log_2\frac{p(\phi,\theta)}{f(\phi)g(\theta)} \quad (5)$$

where *p* is the joint probability distribution function of *X* and *Y*, and *f* and *g* are the marginal probability distribution functions of *X* and *Y* respectively, I is normalized by *B*, the number of histogram bins used to construct *f* and *g*.

Another measure of coherence between the two time series is the angle strength of the phase angle difference between the series, also known as the mean phase coherence, ρ:

$$\rho = \frac{1}{N}\sqrt{\sum_{t=1}^{N}\cos^2(\phi_t-\theta_t)+\sum_{t=1}^{N}\sin^2(\phi_t-\theta_t)} \quad (6)$$

We can search for the optimum relative phase delay between the two series by lagging one time series relative to the other by a phase lag, Δ, in both (5) and (6).

3 Data

We used a 135-year time series of the monthly SOI (Ropelewski and Jones, 1987), as the atmospheric component of ENSO and the Niño3 SST index (1857-2001) (Kaplan, Cane, Kushnir, Clement, Blumenthal and Rajagopalan, 1998), defined as the monthly SST averaged over the eastern half of the tropical Pacific (5ºS-5ºN, 90º -150ºW) as the oceanic part. To ensure the robustness of the results, we repeated the analyses for the monthly Niño1+2 (0º - 10ºS, 90º -80ºW) and monthly Niño3.4 (5ºS- 5ºN, 170º -120ºW) time series (Kaplan et al., 1998). Northern Hemisphere annular mode (NAM) was represented by the monthly AO index based on the pressure pattern (1899-2001) (Thompson and Wallace, 1998) and the extended AO index (1857-1997) based on the pattern of surface air temperature anomalies (Thompson and Wallace, 1998).

Ice condition in NH were represented by maximum annual ice extent in the Baltic Sea (BMI), 1857-2000 (Seinä and Palosuo, 1996), April ice extent in the Barents Sea (BE: Eastern part 10º- 70ºE; and BW: Western part 30ºW- 10ºE), 1864-1998 (Venje, 2001) and the date of ice break-up at Riga since 1857 (Jevrejeva and Moore, 2001). Global SST since 1854 were taken from the ERSST (Smith and Reynolds, 2003) 2°x2° dataset down-sampled to yearly values.

4 Results

Results from wavelet coherence (Figure 1) show that relationship between ENSO and NH ice conditions is relatively weak and varies considerably with time. Figures 1 a,b demonstrate that the relationship between ice conditions and AO is not stationary and the influence of AO has generally increased over the last 60 years over a broadening spectrum of periods. There is evidence of a shift in the period of maximum coherence from the 2.2- 5.2 to the 3.5-7.8 and 12-20 year band for the Baltic sea after 1920. Slightly weaker ENSO influence on the variability of ice conditions associated with 2.2- 3.5, 5.2-7.8 and 12-20 year signals, with noticeable increase in the 12-20 year band after 1920 is shown on Figure 1 c,d.

Robustness of coupling via 2.2-5.7 year signals is examined by phase dynamics modeling. For this analysis we use the average mutual information (5) and mean phase coherence (6). We firstly filter both time series with a Paul wavelet centred on 3 and 5 years. The peak in I and ρ is at 0-3 months with SOI leading Niño3 and Barents sea ice conditions, Niño3 leading Barents sea ice conditions for the 3-year signals (Jevrejeva et al, 2004). The ENSO influence via 12-20 year signals is maximal for 2-5 year lag (not shown here).

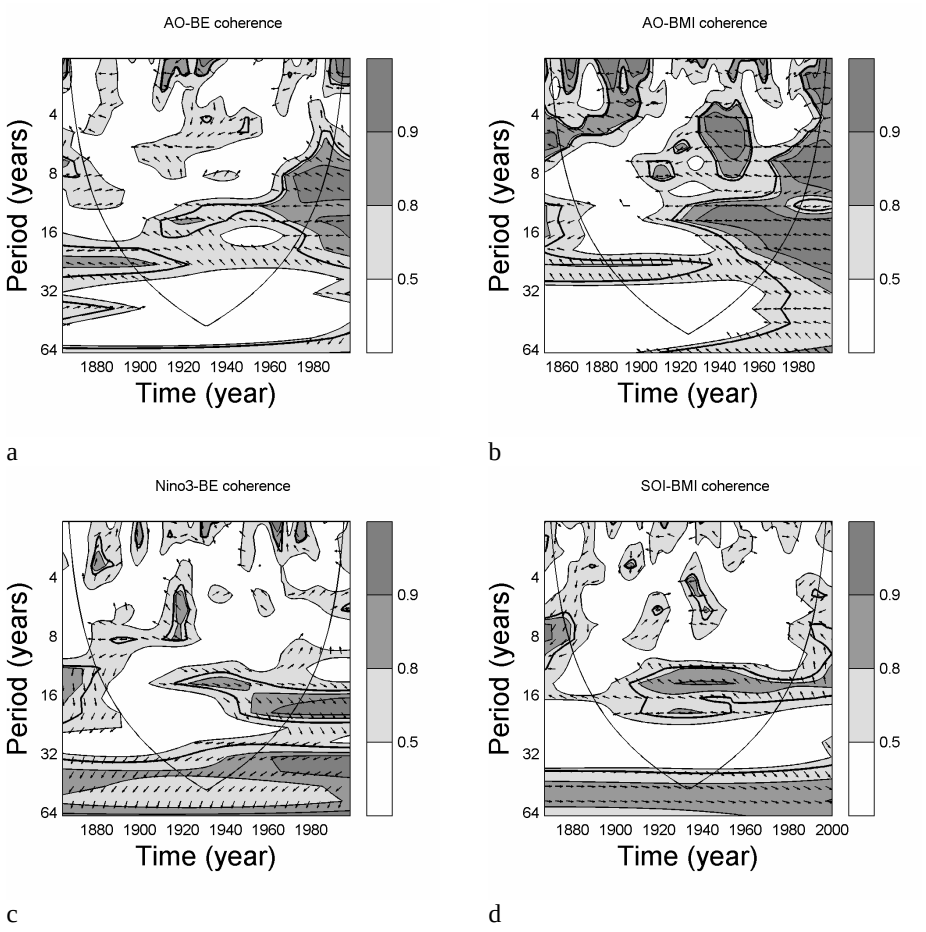

Figure 1. The wavelet coherency and phase difference between the AO/Barents sea ice extent (a). Contours are wavelet squared coherencies. The vectors indicate the phase difference (a horizontal arrow pointing from left to right signifies in-phase and an arrow pointing vertically upward means the second series lags the first by 90 degrees (i.e. the phase angle is 270º); b) the same for the AO/ice extent in the Baltic Sea; c) the same for the Niño3/ice extent in the Barents Sea; d) the same for the SOI/ice extent in the Baltic Sea.

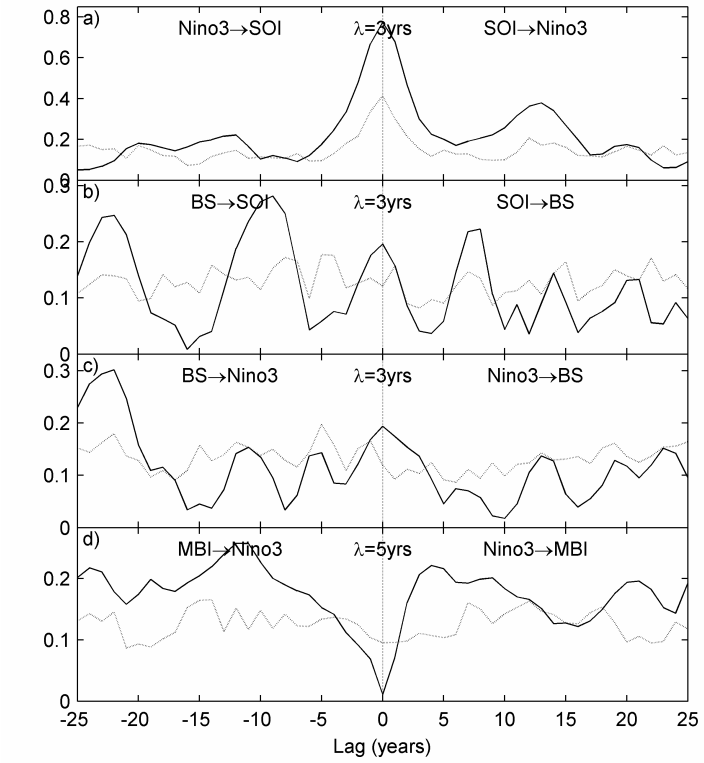

Figure 2. Relationships between time series that have been Paul wavelet filtered with centre frequency λ, expressed as average mutual information, (I), (dotted curves), and mean phase coherence, ρ, (solid line) as a function of the phase lag (Δ) between the series for a) SOI and Niño3, b) SOI and Barents sea ice conditions, c) Niño3 and Barents sea ice conditions, d) Niño3 and Baltic sea ice conditions.

The different phase relationship between signals with periodicities of 2.2-5.7 and those of 12-20 years suggests different mechanisms of signal propagation from the equatorial Pacific Ocean to the polar regions for the decadal-scale signals and for the sub-decadal ones. Similar results are revealed by Jevrejeva et al. (2004). The 2.2- 5.7 year signals are most likely transmitted via the stratosphere, and the AO mediating propagation of the signals, through coupled stratospheric and tropospheric circulation variability that accounts for vertical planetary wave propagation. The connection between the QB oscillations (2.2-3.5 years) detected in ice conditions time series and in tropical forcing, has been described by Baldwin and Dunkerton (2001), as extra-tropical wave propagation, affecting breakdown of the wintertime

stratospheric polar vortices. Since the AO may be interpreted as a physical phenomenon associated with the structure of the polar vortex and related changes in the stratospheric and tropospheric pressure fields and the stratospheric polar vortex affects surface weather patterns, the QBO has an effect on high latitude weather patterns (Baldwin and Dunkerton, 2001; Castanheira and Graf, 2003).

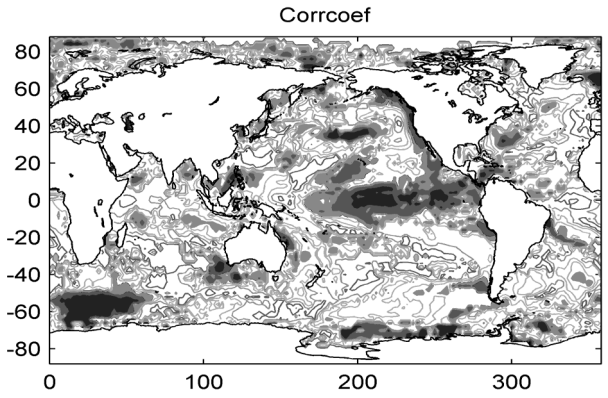

a

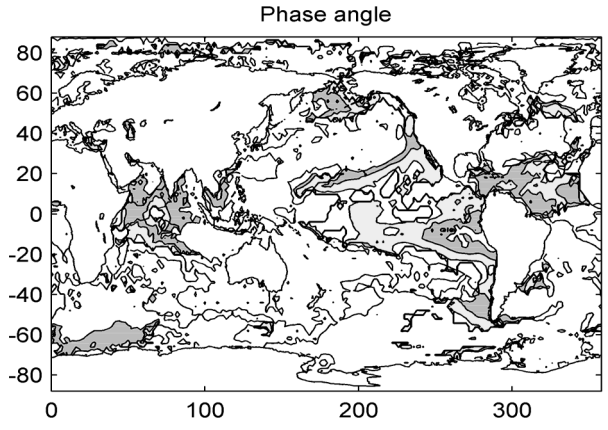

b

Figure 3. Map (a) of magnitude of correlation between SST and the in-phase and quadrature 13.9 year SOI cycle. Dark grey (r = 0.7) and light grey (r = 0.6) and grey (r = 0.5) correspond to the area where the correlation coefficients are maximum. Map (b) of relative phase angle between the low-pass filtered (wavelength>10years) SST and in-phase and quadrature SOI 13.9 year cycle. Dark grey corresponds to the delay of about 2.5-3.0 years, light grey is area where the delay is about 1.5-2.0 year.

Jevrejeva et al. (2004) demonstrate that the delay of about two years in the 13.9 year signals detected in polar region can be explained by the transit time of the 13.9 year signal associated with equatorial coupled ocean (0.13-0.17 ms-1) propagation in the Pacific ocean (White, Tourre, Barlow and Dettinger, 2003), boundary Kelvin waves (1-3 ms-1) propagation along the western margins of the Americas (Meyers, Melsom, Mitchum and O'Brien, 1998) and by poleward-propagating of atmospheric angular momentum (Dickey, Marcus and Viron, 2003).

We have projected the 13.9 year signal extracted from SOI on the SST anomalies, which have been low-pass filtered (wavelength>10years) in order to remove typical 2.2-5.7 year ENSO signals SST (1854-1997) (Figure 3). The strength of correlation and the phase of correlation maps illustrate a meridional V-shape pattern in Pacific, which is symmetric along the equator, propagating eastward across the ocean and we can trace the propagation along the western margin of South and North America and also along the Arctic continental shelf as well as along Antarctica. The strongest effect is observed in polar regions.

5 Conclusion

We provide observational evidence of ENSO influence on the winter climate variability in NH during the last 135 years via signals in the 2.2, 3.5, 5.7 and 13.9 year bands. The presence of coupling between ENSO and NH ice conditions is revealed with use of wavelet coherence, average mutual information and mean phase coherence methods.

Phase relationships for the different frequency signals suggest that there are different mechanisms (fast and slow) for distribution of the 2.2-5.7 year and the 13.9 year signals. The 2.2- 5.7 year signals are most likely transmitted via the stratosphere, and the AO mediating propagation of the signals, through coupled stratospheric and tropospheric circulation variability that accounts for vertical planetary wave propagation. Low frequency variability (12-20 years) is more likely associated with an oceanic origin. The delay of about two years in the 13.9 year signals from Barents and Baltic Seas can be explained by long-lived ENSO events in the Pacific Ocean.

References

Baldwin, M.P. and Dunkerton, T.J. (2001) Stratospheric Harbingers of Anomalous Weather Regimes, *Science*, 294, 581-584.

Castanheira, J.M. and Craf, H.-F. (2003) North Pacific-North Atlantic relationships under stratospheric control?, *J. Geophys. Res*., 108, 4036, 10.1029/2002JD002754.

Dickey, J.O., S.L. Marcus and Viron, O. (2003) Coherent interannual and decadal variations in the atmosphere-ocean system, *Geophys. Res. Let*, 30, 2002GL016763.

Foufoula-Georgiou, E. and Kumar, K. (1995) *Wavelets in Geophysics*, Academic Press, 373.

Gloersen, R. 1995. Modulation of hemispheric sea-ice cover by ENSO events, *Nature*, 373, 503-505.

Grinsted, A., J. C. Moore and Jevrejeva, S. (2004) Application of the cross wavelet transform and wavelet coherence to geophysical time series, *Nonlinear Processes in Geophysics*, 11, 561-566.

Huang, J., K. Higuchi and Shabbar, A. (1998) The relationship between the North Atlantic Oscillation and the ENSO, *Geophys. Res. Let.*, 25, 2707-2710.

Jevrejeva, S. and Moore, J.C. (2001) Singular Spectrum Analysis of Baltic Sea ice conditions and large-scale atmospheric patterns since 1708, *Geophys. Res. Let.*, 28, 4503-07.

Jevrejeva, S., J. C. Moore and Grinsted, A. (2003) Influence of the arctic oscillation and El Nino-Southern Oscillation (ENSO) on ice conditions in the Baltic Sea: The wavelet approach, *J. Geophys. Res*., 108, 2003JD003417.

Jevrejeva, S., J.C. Moore and Grinsted, A. (2004) Oceanic and atmospheric transport of multi-year ENSO signatures to the polar regions. *Geophys. Res. Lett.*, 31, L24210, doi:10.1029/2004GL020871.

Kaplan, A., M. A. Cane, Y. Kushnir, A.C. Clement, M.B. Blumenthal and Rajagopalan, B. (1998) Analyses of global sea surface temperature 1856-1991, *J. Geophys. Res.*, 103, 18567-18589.

Merkel, U. and Latif, M. (2002) A high resolution AGCM study of the El Niño impact on the North Atlantic/European sector, *Geophys. Res. Let.*, 29, 2001GLO13726.

Meyers, S.D., A. Melsom, G.T. Mitchum and O'Brien, J.J. (1998) Detection of the fast Kelvin waves teleconnection due to El Niño Southern Oscillation, *J. Geophys. Res.*, 103, 27655-27663.

Mokhov, I. I. and Smirnov, D. A. (2006) El Niño–Southern Oscillation drives North Atlantic Oscillation as revealed with nonlinear techniques from climatic indices *Geophys. Res. Lett*., 33, L03708 10.1029/2005GL024557

Papoulis, A. (1984) *Probability, Random Variables, and Stochastic Processes*, second edition. New York: McGraw-Hill, *(See Chapter 15.)*

Pozo-Vázquez, D., M.J. Esteban-Parra, F.S. Rodrigo and Castro-Diez, Y. (2001) The association between ENSO and winter atmospheric circulation and temperature in the North Atlantic Region, *J. Clim.*, 14, 3408-3420.

Ribera, P., and Mann, M. (2002) Interannual variability in the NCEP reanalysis 1948-1999, *Geophys. Res. Let*., 29, 2001GL013905.

Ropelewski, C.F., and Jones, P.D. (1987) An extension of the Tahiti-Darwin Southern Oscillation Index, *Monthly Weather Review, 115*, 2161-2165.

Seinä, A. and Palosuo, E. (1996) The classification of the maximum annual extent of ice cover in the Baltic Sea 1720-1995", *Report series of the Finnish Institute of Marine Research* No 27, 79-91.

Smith, T.M. and Reynolds, R.W. (2003). Extended Reconstruction of Global Sea Surface Temperatures Based on COADS Data (1854-1997), *J. Clim.*, 16, 1495-1510.

Thompson, D.W.J. and Wallace, J.M. (1998) The Arctic Oscillation signature in the winter geopotential height and temperature fields, *Geophys. Res. Let*., *25*, 1297-1300.

Torrence, C. and Compo, G. P. (1998) A practical guide to wavelet analysis, *Bull. Am. Meteorol. Soc.*, 79, 61–78.

Torrence, C. and Webster, P. (1999) Interdecadal Changes in the ENSO-Monsoon System, *J.Clim.*, 12, 2679-2690.

Venegas, S.A. and Mysak, L.A. (2000) Is there a dominant timescale of natural climate variability in the Arctic?, *J. Clim.*, 13, 3412-3434.

Venje, T. (2001) Anomalies and trends of sea ice extent and atmospheric circulation in the Nordic Seas during the period 1864-1998, *J. Clim.*, 14, 255-267.

White, W.B., Y.M. Tourre, M. Barlow, and Dettinger, M. (2003) A delayed action oscillator shared by biennial, interannual, and decadal signals in the Pacific Basin, *J. Geophys. Res.*, 108, 2002JC001490.

White, W.B. and Tourre, Y. M. (2003) Global SST/SLP waves during the 20th century, *Geophys. Res. Let*, 30, 2003JL017055.